# COLD POSTERIORS THROUGH PAC-BAYES

**Anonymous authors**
Paper under double-blind review

## ABSTRACT

We investigate the cold posterior effect through the lens of PAC-Bayes generalization bounds. We argue that in the non-asymptotic setting, when the number of training samples is (relatively) small, discussions of the cold posterior effect should take into account that approximate Bayesian inference does not readily provide guarantees of performance on out-of-sample data. Instead, out-of-sample error is better described through a generalization bound. In this context, we explore the connections of the ELBO objective from variational inference and the PAC-Bayes objectives. We note that, while the ELBO and PAC-Bayes objectives are similar, the latter objectives naturally contain a temperature parameter $\lambda$ which is not restricted to be $\lambda = 1$. For both regression and classification tasks, in the case of isotropic Laplace approximations to the posterior, we show how this PAC-Bayesian interpretation of the temperature parameter captures important aspects of the cold posterior effect.

## 1 INTRODUCTION

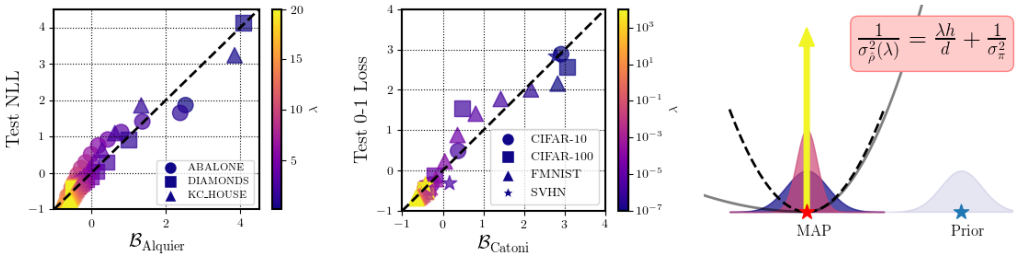


(a) Regression tasks (b) Classification tasks (c) Laplace, different temperatures $\lambda$

Figure 1: PAC-Bayes bounds correlate with the test negative log-likelihood (NLL) and the test 0-1 Loss for different values of the temperature $\lambda$ (quantities on both axes are normalized). (a) Regression tasks on UCI Abalone, UCI Diamonds, and KC_House datasets (prior variance $\sigma_\pi^2 = 0.005$, 2-layer MLP). (b) Classification tasks on CIFAR-10, CIFAR-100, and SVHN datasets ($\sigma_\pi^2 = 0.1$, ResNet22) and FMNIST dataset ($\sigma_\pi^2 = 0.1$, ConvNet). (c) Graphical representation of the Laplace approximation for different temperatures: for hot temperatures $\lambda \ll 1$, the posterior variance becomes equal to the prior variance; for $\lambda = 1$ the posterior variance is regularized according to the curvature $h$; for cold temperatures $\lambda \gg 1$, the posterior becomes a Dirac delta on the MAP estimate.

In their influential paper, Wenzel et al. (2020) highlighted the observation that Bayesian neural networks typically exhibit better test time predictive performance if the posterior distribution is "sharpened" through tempering. Their work has been influential primary because it serves as a well documented example of the potential drawbacks of the Bayesian approach to deep learning. While other subfields of deep learning have seen rapid adoption, and have had impact on real world problems, Bayesian deep learning has, to date, seen relatively limited practical use (Izmailov et al., 2021; Lotfi et al., 2022; Dusenberry et al., 2020; Wenzel et al., 2020). The "cold posterior effect", as the authors of Wenzel et al. (2020) named their observation, highlights an essential mismatch between Bayesian theory and practice. As the number of training samples increases, Bayesian theory tells states that the posterior distribution should be concentrating more and more on the true model parameters, in a frequentist sense. At any time, the posterior is our best guess at the true model

parameters, without having to resort to heuristics. Since the original paper, a number of works (Noci et al., 2021; Zeno et al., 2020; Adlam et al., 2020; Nabarro et al., 2022; Fortuin et al., 2021; Aitchison, 2020) have attempted to explain the cold posterior effect, identify its origins, propose remedies and defend Bayesian deep learning in the process.

The experimental setups where the cold posterior effect arises have, however, been hard to pinpoint precisely. Noci et al. (2021) conducted detailed experiments testing various hypotheses. The cold posterior effect was shown to arise from augmenting the data during optimization (data augmentation hypothesis), from selecting only the "easiest" data samples when constructing the dataset (data curation hypothesis), and from selecting a "bad" prior (prior misspecification hypothesis). Nabarro et al. (2022) propose a principled log-likelihood that incorporates data augmentation, however they show that the cold-posterior persists. Bachmann et al. (2022) also propose a mechanism by which data-augmentation leads to mispecification and how the tempered posterior alleviates it. They prove their results for simplified settings, and acknowledge that there might be other potential sources of the cold-posterior effect. Data curation was first proposed as an explanation in Aitchison (2020), however the author shows that data curation can only explain a part of the cold posterior effect. Misspecified priors have also been explored as a possible cause in several other works (Zeno et al., 2020; Adlam et al., 2020; Fortuin et al., 2021). Again the results have been mixed. In smaller models, data dependent priors seem to decrease the cold posterior effect while in larger models the effect increases (Fortuin et al., 2021).

We posit that discussions of the cold posterior effect should take into account that in the *non-asymptotic setting* (where the number of training data points is relatively small), Bayesian inference does not readily provide a guarantee for *performance on out-of-sample data*. Existing theorems describe *posterior contraction* (Ghosal et al., 2000; Blackwell & Dubins, 1962), however in practical settings, for a finite number of training steps and for finite training data, it is often difficult to *precisely* characterise how much the posterior concentrates. Furthermore, theorems on posterior contraction are somewhat unsatisfying in the supervised classification setting, in which the cold posterior effect is usually discussed. Ideally, one would want a theoretical analysis that links the posterior distribution to the *test* error directly.

Here, we investigate PAC-Bayes generalization bounds (McAllester, 1999; Catoni, 2007; Alquier et al., 2016; Dziugaite & Roy, 2017) as the model that governs performance on out-of-sample data. PAC-Bayes bounds describe the performance on out-of-sample data, through an application of the convex duality relation between measurable functions and probability measures. The convex duality relationship naturally gives rise to the log-Laplace transform of a special random variable (Catoni, 2007). Importantly the log-Laplace transform has a temperature parameter $\lambda$ which is not constrained to be $\lambda = 1$. We investigate the relationship of this temperature parameter to cold posteriors.

In summary, our contributions are the following:

- Through detailed experiments, for regression and classification tasks, and for the Laplace approximation to the posterior, we show that PAC-Bayes bounds correlate with out-of-sample performance for different values of the temperature parameter $\lambda$. This might indicate that the temperature in the cold-posterior literature coincides with the temperature of the log-Laplace transform.
- We find that the coldest temperature (such that the posterior is a Dirac delta centered on a MAP estimate of the weights) is empirically always optimal in terms of test accuracy. However, the same does not hold true for the negative log-likelihood. This highlights that the evaluation metric choice plays an important role when discussing the cold-posterior effect. Separately, our results raise important questions about the Laplace approximation for Bayesian inference in deep learning.
- We derive a PAC-Bayes bound for the case of the widely used generalized Gauss–Newton Laplace approximations to the posterior. Our bound implies that different factors such as the curvature at the minimum and the prior interact in a complex way and might result in different optimal temperatures $\lambda$. This might explain why it is difficult to pinpoint an exact cause for the cold-posterior effect.

We also include a detailed FAQ section in the Appendix.

## 2 COLD POSTERIOR EFFECT: MISSPECIFIED AND NON-ASYMPTOTIC SETTING

We denote the learning sample $(X, Y) = \{(\boldsymbol{x}_i, y_i)\}_{i=1}^n \in (\mathcal{X} \times \mathcal{Y})^n$, that contains $n$ input-output pairs. Observations $(X, Y)$ are assumed to be sampled randomly from a distribution $\mathcal{D}$. Thus, we denote $(X, Y) \sim \mathcal{D}^n$ the i.i.d observation of $n$ elements. We consider loss functions $\ell : \mathcal{F} \times \mathcal{X} \times \mathcal{Y} \to \mathbb{R}$, where $\mathcal{F}$ is a set of predictors $f : \mathcal{X} \to \mathcal{Y}$. We also denote the risk $\mathcal{L}^{\ell}_{\mathcal{D}}(f) = \mathbf{E}_{(\boldsymbol{x},y)\sim\mathcal{D}}\ell(f, \boldsymbol{x}, y)$ and the empirical risk $\hat{\mathcal{L}}^{\ell}_{X,Y}(f) = (1/n)\sum_i \ell(f, \boldsymbol{x}_i, y_i)$. We consider two probability measures, the prior $\pi \in \mathcal{M}(\mathcal{F})$ and the posterior $\hat{\rho} \in \mathcal{M}(\mathcal{F})$. Here, $\mathcal{M}(\mathcal{F})$ denotes the set of all probability measures on $\mathcal{F}$. We encounter cases where we make predictions using the posterior predictive distribution $\mathbf{E}_{f\sim\hat{\rho}}[p(y|\boldsymbol{x}, f)]$. We will use two loss functions, the non-differentiable zero-one loss $\ell_{01}(f, \boldsymbol{x}, y) = \mathbb{I}(\arg\max_j f(\boldsymbol{x})_j \neq y)$, and the negative log-likelihood, which is a commonly used differentiable surrogate $\ell_{\text{nll}}(f, \boldsymbol{x}, y) = -\log(p(y|\boldsymbol{x}, f))$, where we assume that the outputs of $f$ are normalized to form a probability distribution. Given the above, the Evidence Lower Bound (ELBO) has the following form

$$-\mathbf{E}_{f\sim\hat{\rho}}\hat{\mathcal{L}}^{\ell_{\text{nll}}}_{X,Y}(f) - \frac{1}{\lambda n}\text{KL}(\hat{\rho}\|\pi), \tag{1}$$

where $\lambda = 1$. Note that our temperature parameter $\lambda$ is the *inverse* of the one typically used in cold posterior papers. In this form $\lambda$ has a clearer interpretation as the temperature of a log-Laplace transform. Overall our setup is one of the cases discussed in Wenzel et al. (2020), p3 Section 2.3. While they use MCMC to conduct their experiments, we opt for the ELBO for analytical tractability. Wenzel et al. (2020) also temper by $\lambda$ both the likelihood and the prior in the MCMC inference setting. As discussed in Aitchison (2020) and Wenzel et al. (2020) the relevant setting for the ELBO is the one we consider (Eq. 1), where only the KL is tempered. One then typically models the posterior and prior distributions over weights using a parametric distribution (commonly a Gaussian) and optimizes the ELBO, using the reparametrization trick, to find the posterior distribution (Blundell et al., 2015; Khan et al., 2018; Mishkin et al., 2018; Ashukha et al., 2019; Wenzel et al., 2020). The cold posterior is the following observation:

> *Even though the ELBO has the form (1) with $\lambda = 1$, practitioners have found that much larger values $\lambda \gg 1$ typically result in better test time performance, for example a lower test misclassification rate and lower test negative log-likelihood.*

The starting point of our discussion will be thus to define the quantity that we care about in the context of Bayesian deep neural networks and cold posterior analyses. Concretely, in the setting of supervised prediction, what we often try to minimize is

$$\text{KL}(p_{\mathcal{D}}(y|\boldsymbol{x})\|\mathbf{E}_{f\sim\hat{\rho}}[p(y|\boldsymbol{x}, f)]) = \mathbf{E}_{\boldsymbol{x},y\sim\mathcal{D}}\left[\ln\frac{p_{\mathcal{D}}(y|\boldsymbol{x})}{\mathbf{E}_{f\sim\hat{\rho}}[p(y|\boldsymbol{x}, f)]}\right], \tag{2}$$

the conditional relative entropy (Cover, 1999) between the true conditional distribution $p_{\mathcal{D}}(y|\boldsymbol{x})$ and the posterior predictive distribution $\mathbf{E}_{f\sim\hat{\rho}}[p(y|\boldsymbol{x}, f)]$. For example, this is implicitly the quantity that we minimize when optimizing classifiers using the cross-entropy loss (Masegosa, 2020; Morningstar et al., 2022). It is also on this and similar predictive metrics that the cold posterior appears. In the following we will outline the relationship between the ELBO, PAC-Bayes and (2).

### 2.1 ELBO

We assume a training sample $(X, Y) \sim \mathcal{D}^n$ as before, denote $p(\mathbf{w}|X, Y)$ the true posterior probability over predictors $f$ parameterized by $\mathbf{w}$ (typically weights for neural networks), and $\pi$ and $\hat{\rho}$ respectively the prior and variational posterior distributions as before. The ELBO results from the following calculations

$$\begin{aligned}
\text{KL}(\hat{\rho}(\mathbf{w})\|p(\mathbf{w}|X, Y)) &= \int \hat{\rho}(\mathbf{w})\ln\frac{\hat{\rho}(\mathbf{w})}{p(\mathbf{w}|X, Y)}d\mathbf{w} = \int \hat{\rho}(\mathbf{w})\ln\frac{\hat{\rho}(\mathbf{w})p(Y|X)}{\pi(\mathbf{w})p(Y|X, \mathbf{w})}d\mathbf{w} \\
&= \int \hat{\rho}(\mathbf{w})\left[-\ln p(Y|X, \mathbf{w}) + \ln\frac{\hat{\rho}(\mathbf{w})}{\pi(\mathbf{w})} + \ln p(Y|X)\right]d\mathbf{w} \\
&= -n\underbrace{\left(-\mathbf{E}_{f\sim\hat{\rho}}\hat{\mathcal{L}}^{\ell_{\text{nll}}}_{X,Y}(f) - \frac{1}{n}\text{KL}(\hat{\rho}\|\pi)\right)}_{\text{ELBO}} + \ln p(Y|X).
\end{aligned}$$

Thus, maximizing the ELBO can be seen as minimizing the KL divergence between the true posterior and the variational posterior over the weights $\mathrm{KL}(\hat{\rho}(\mathbf{w})\|p(\mathbf{w}|X,Y))$. The true posterior distribution $p(\mathbf{w}|X,Y)$ gives more probability mass to predictors which are more likely given the training data, however these predictors do not necessarily minimize $\mathrm{KL}(p_{\mathcal{D}}(y|\boldsymbol{x})\|\mathbf{E}_{f\sim\hat{\rho}}[p(y|\boldsymbol{x},f)])$, the evaluation metric of choice (2) for supervised prediction. In the well-specified regime (where the true predictor $f^*$ is $f^* \in \mathcal{F}$) and when $n \to \infty$, the Blackwell–Dubins consistency theorem (Blackwell & Dubins, 1962) implies that the posterior quickly concentrates on the true set of parameters. In such cases, a more detailed analysis, such as a PAC-Bayesian one, is unnecessary as the posterior is akin to a Dirac delta mass at the true parameters. However neural networks do not operate in this regime. The existence of multiple minima hints that neural networks are misspecified, and the number of samples is small relative to the number of parameters.

Operating in the regime where $f^* \notin \mathcal{F}$ and where $n$ is (comparatively) small makes it important to derive a more precise certificate of generalization through a generalization bound, which directly bounds the true risk. In the following we focus on analyzing a PAC-Bayes bound in order to obtain insights into when the cold posterior effect occurs.

### 2.2 PAC-Bayes

We first look at the following bound, that we name "Alquier" bound and denote by $\mathcal{B}_{\mathrm{Alquier}}$.

**Theorem 1** ($\mathcal{B}_{\mathrm{Alquier}}$, Alquier et al., 2016)**.** *Given a distribution $\mathcal{D}$ over $\mathcal{X}\times\mathcal{Y}$, a hypothesis set $\mathcal{F}$, a loss function $\ell : \mathcal{F}\times\mathcal{X}\times\mathcal{Y}\to\mathbb{R}$, a prior distribution $\pi$ over $\mathcal{F}$, real numbers $\delta\in(0,1]$ and $\lambda>0$, with probability at least $1-\delta$ over the choice $(X,Y)\sim\mathcal{D}^n$, we have for all $\hat{\rho}$ on $\mathcal{F}$*

$$\mathbf{E}_{f\sim\hat{\rho}}\mathcal{L}^{\ell}_{\mathcal{D}}(f) \le \mathbf{E}_{f\sim\hat{\rho}}\hat{\mathcal{L}}^{\ell}_{X,Y}(f) + \frac{1}{\lambda n}\left[\mathrm{KL}(\hat{\rho}\|\pi) + \ln\frac{1}{\delta} + \Psi_{\ell,\pi,\mathcal{D}}(\lambda,n)\right]$$

$$\textit{where } \Psi_{\ell,\pi,\mathcal{D}}(\lambda,n) = \ln \mathbf{E}_{f\sim\pi}\mathbf{E}_{X',Y'\sim\mathcal{D}^n}\exp\left[\lambda n\left(\mathcal{L}^{\ell}_{\mathcal{D}}(f) - \hat{\mathcal{L}}^{\ell}_{X',Y'}(f)\right)\right].$$

There are three different terms in the above bound. The empirical risk term $\mathbf{E}_{f\sim\hat{\rho}}\hat{\mathcal{L}}^{\ell}_{X,Y}(f)$ is the empirical mean of the loss of the classifier over all training samples. The KL term $1/(\lambda n)\mathrm{KL}(\hat{\rho}\|\pi)$ is the complexity of the model, which in this case is measured as the KL-divergence between the posterior and prior distributions. The Moment term $1/(\lambda n)\Psi_{\ell,\pi,\mathcal{D}}(\lambda,n)$, this is the log-Laplace transform for a reversal of the temperature, we will keep the name "Moment" in the following. Using a PAC-Bayes bound together with Jensen's inequality, one can bound (2) directly as follows

$$\begin{aligned}
&\mathrm{KL}(p_{\mathcal{D}}(y|\boldsymbol{x})\|\mathbf{E}_{f\sim\hat{\rho}}[p(y|\boldsymbol{x},f)]) = \mathbf{E}_{\boldsymbol{x},y\sim\mathcal{D}}\left[\ln\frac{p_{\mathcal{D}}(y|\boldsymbol{x})}{\mathbf{E}_{f\sim\hat{\rho}}[p(y|\boldsymbol{x},f)]}\right]\\
&= \mathbf{E}_{\boldsymbol{x},y\sim\mathcal{D}}[-\ln\mathbf{E}_{f\sim\hat{\rho}}[p(y|\boldsymbol{x},f)]] + \mathbf{E}_{\boldsymbol{x},y\sim\mathcal{D}}[\ln p_{\mathcal{D}}(y|\boldsymbol{x})]\\
&\le \mathbf{E}_{\boldsymbol{x},y\sim\mathcal{D}}[\mathbf{E}_{f\sim\hat{\rho}}[-\ln p(y|\boldsymbol{x},f)]] + \mathbf{E}_{\boldsymbol{x},y\sim\mathcal{D}}[\ln p_{\mathcal{D}}(y|\boldsymbol{x})]\\
&\le \underbrace{\mathbf{E}_{f\sim\hat{\rho}}\hat{\mathcal{L}}^{\ell_{\mathrm{nll}}}_{X,Y}(f) + \frac{1}{\lambda n}\left[\mathrm{KL}(\hat{\rho}\|\pi) + \ln\frac{1}{\delta} + \Psi_{\ell_{\mathrm{nll}},\pi,\mathcal{D}}(\lambda,n)\right]}_{\text{PAC-Bayes}} + \mathbf{E}_{\boldsymbol{x},y\sim\mathcal{D}}[\ln p_{\mathcal{D}}(y|\boldsymbol{x})].
\end{aligned}$$

The last line holds under the conditions of Theorem 1 and in particular with probability at least $1-\delta$ over the choice $(X,Y)\sim\mathcal{D}^n$. Notice here the presence of the temperature parameter $\lambda\ge 0$, which need not be $\lambda = 1$.

> *In particular it is easy to see that maximizing the ELBO is equivalent to minimizing a PAC-Bayes bound for $\lambda = 1$, which might not necessarily be optimal for a finite sample size. More specifically even for exact inference, where $\mathbf{E}_{\mathbf{w}\sim\hat{\rho}}[p(y|\boldsymbol{x},\mathbf{w})]|_{\hat{\rho}=p(\mathbf{w}|X,Y)} = p(y|\boldsymbol{x},X,Y)$, the Bayesian posterior predictive distribution does not necessarily minimize $\mathrm{KL}(p_{\mathcal{D}}(y|\boldsymbol{x})\|\mathbf{E}_{f\sim\hat{\rho}}[p(y|\boldsymbol{x},f)])$.*

### 2.3 Classification tasks

For classification tasks, we are typically mainly interested in achieving low expected zero-one risk $\mathbf{E}_{f\sim\hat{\rho}}\mathcal{L}^{\ell_{01}}_{\mathcal{D}}(f)$. The ELBO objective is not directly related to this risk, however in the PAC-Bayesian

literature there exist bounds specifically adapted to it. In the following we will use one of the tightest and most commonly used bounds, the "Catoni" bound, denoted $\mathcal{B}_{\text{Catoni}}$.

**Theorem 2** ($\mathcal{B}_{\text{Catoni}}$, Catoni, 2007)**.** *Given a distribution $\mathcal{D}$ over $\mathcal{X} \times \mathcal{Y}$, a hypothesis set $\mathcal{F}$, the 0-1 loss function $\ell_{01} : \mathcal{F} \times \mathcal{X} \times \mathcal{Y} \to [0, 1]$, a prior distribution $\pi$ over $\mathcal{F}$, a real number $\delta \in (0, 1]$, and a real number $\lambda > 0$, with probability at least $1 - \delta$ over the choice of $(X, Y) \sim \mathcal{D}^n$, we have*

$$\forall \hat{\rho} \text{ on } \mathcal{F} : \mathbf{E}_{f\sim\hat{\rho}} \mathcal{L}^{\ell_{01}}_{\mathcal{D}}(f) \leq \Phi^{-1}_{\lambda} \left( \mathbf{E}_{f\sim\hat{\rho}} \hat{\mathcal{L}}^{\ell_{01}}_{X,Y}(f) + \frac{1}{\lambda n} \left[ \text{KL}(\hat{\rho}||\pi) + \ln \frac{1}{\delta} \right] \right), \tag{3}$$

*where* $\Phi^{-1}_{\lambda}(x) = \frac{1-e^{-\lambda x}}{1-e^{-\lambda}}$.

Similarly to the Alquier bound, the empirical risk term is the empirical mean of the loss of the classifier over all training samples. The KL term is the complexity of the model, which in this case is measured as the KL-divergence between the posterior and prior distributions. The Moment term has been absorbed in this case in the function $\Phi^{-1}_{\lambda}(x) = \frac{1-e^{-\lambda x}}{1-e^{-\lambda}}$.

### 2.4 Safe-Bayes and other relevant work

Germain et al. (2016) were the first to find connections between PAC-Bayes and Bayesian inference. However they only investigate the case where $\lambda = 1$. After identifying two sources of misspecification, Grünwald & Langford (2007) proposed a solution, through an approach which they named Safe-Bayes (Grünwald, 2012; Grünwald & Van Ommen, 2017). Safe-Bayes corresponds to finding a temperature parameter $\lambda$ for a generalized (tempered) posterior distribution with $\lambda$ possibly different than 1. The optimal value of $\lambda$ is found by taking a sequential view of Bayesian inference, and for a Cèsaro averaged posterior, which is an average of the posteriors at different optimization steps, and which doesn't coincide with the standard posterior. The analysis of Grünwald (2012); Grünwald & Van Ommen (2017) is also restricted to the case where $\lambda < 1$. By contrast we provide an analytical expression of the bound on true risk, given $\lambda$, and also numerically investigate the case of $\lambda > 1$. Our analysis thus provides intuition regarding which parameters (for example the curvature) might result in cold posteriors. Catoni (2007) discusses the optimal value of the temperature $\lambda$ for PAC-Bayes bounds, for *fixed* priors and posteriors. By contrast we investigate the case where the posterior is optimized for different $\lambda$ and which is the relevant one for the cold-posterior literature.

## 3 Experiments on regression and classification tasks

The ELBO (1) is minimized at the probability density $\rho^\star(f)$ given by: $\rho^\star(f) := \pi(f) e^{-\lambda n \hat{\mathcal{L}}^{\ell_{\text{nll}}}_{X,Y}(f)} / \mathbf{E}_{f\sim\pi} \left[ e^{-\lambda n \hat{\mathcal{L}}^{\ell_{\text{nll}}}_{X,Y}(f)} \right]$ (Catoni, 2007). We will use the Laplace approximation to the posterior in our experiments. This is equivalent to approximating $\lambda n \hat{\mathcal{L}}^{\ell_{\text{nll}}}_{X,Y}(f)$ using a second order Taylor expansion around a minimum $\mathbf{w}_{\hat{\rho}}$, such that $\lambda n \hat{\mathcal{L}}^{\ell_{\text{nll}}}_{X,Y}(f_{\mathbf{w}}) \approx \lambda n \hat{\mathcal{L}}^{\ell_{\text{nll}}}_{X,Y}(f_{\mathbf{w}_{\hat{\rho}}}) + \lambda n (\mathbf{w} - \mathbf{w}_{\hat{\rho}})^\top \frac{1}{2} \nabla\nabla \hat{\mathcal{L}}^{\ell_{\text{nll}}}_{X,Y}(f_{\mathbf{w}})|_{\mathbf{w}=\mathbf{w}_{\hat{\rho}}} (\mathbf{w} - \mathbf{w}_{\hat{\rho}})$. Assuming a Gaussian prior $\pi = \mathcal{N}(0, \sigma^2_\pi \mathbf{I})$, the Laplace approximation to the posterior $\hat{\rho}$ is again a Gaussian

$$\hat{\rho} = \mathcal{N} \left( \mathbf{w}_{\hat{\rho}}, \left( \lambda \mathbf{H} + \frac{1}{\sigma^2_\pi} \mathbf{I} \right)^{-1} \right)$$

where $\mathbf{H}$ is the network Hessian $\mathbf{H} = n \nabla\nabla \hat{\mathcal{L}}^{\ell_{\text{nll}}}_{X,Y}(f_{\mathbf{w}})|_{\mathbf{w}=\mathbf{w}_{\hat{\rho}}}$. This Hessian is generally infeasible to compute in practice for modern deep neural networks, such that many approaches employ the generalized Gauss–Newton (GGN) approximation $\mathbf{H}^{\text{GGN}} := \sum_{i=1}^n \mathcal{J}_{\mathbf{w}}(\boldsymbol{x}_i)^\top \mathbf{\Lambda}(\boldsymbol{y}_i; f_i) \mathcal{J}_{\mathbf{w}}(\boldsymbol{x}_i)$, where $\mathcal{J}_{\mathbf{w}}(\boldsymbol{x})$ is the network per-sample Jacobian $[\mathcal{J}_{\mathbf{w}}(\boldsymbol{x})]_c = \nabla_{\mathbf{w}} f_c(\boldsymbol{x}; \mathbf{w}_{\hat{\rho}})$, and $\mathbf{\Lambda}(\boldsymbol{y}; f) = -\nabla^2_{ff} \log p(\boldsymbol{y}; f)$ is the per-input noise matrix (Kunstner et al., 2019). We will use two simplified versions of the GGN

- An isotropic approximation with variance $\sigma^2_{\hat{\rho}}(\lambda)$ such that $\frac{1}{\sigma^2_{\hat{\rho}}(\lambda)} = \frac{\lambda h}{d} + \frac{1}{\sigma^2_\pi}$, where $h = \sum_{i,j,k} g(i,k) (\nabla_{\mathbf{w}} f_k(\boldsymbol{x}_i; \mathbf{w}_{\hat{\rho}})_j)^2$ is the trace of the Gauss–Newton approximation to the Hessian, with $g(i,k) = [\mathbf{\Lambda}(\boldsymbol{y}_i; f)]_{kk}$.

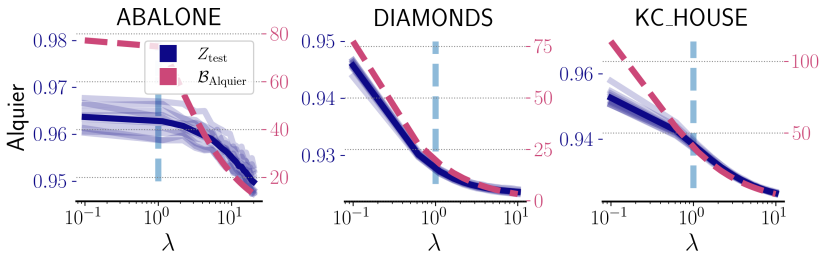


Figure 2: $\mathcal{B}_{\text{Alquier}}$ PAC-Bayes bound and test NLL mean, as well as 10 MAP trials (we denote $\lambda = 1$ by ). For varying $\lambda$ for the regression tasks on the UCI Abalone, UCI Diamonds and KC_House datasets. $\mathcal{B}_{\text{Alquier}}$ bound closely tracks the test NLL. There is a rapid improvement as $\lambda \uparrow$ followed by a slowdown in improvements. Coldest posteriors $\lambda \gg 1$ are always best.

- The Kronecker-Factorized Approximate Curvature (KFAC) (Martens & Grosse, 2015) approximation, which retains only a block diagonal part of the GGN.

When making predictions, we use the posterior predictive distribution $\mathbf{E}_{\mathbf{w}\sim\hat{\rho}}[p(y|\boldsymbol{x}, f_{\mathbf{w}})]$ of the *full neural network model*, meaning that samples from $\hat{\rho}$ are inputted to the full neural network. Since the 0-1 loss is not differentiable, the posterior estimated with the cross entropy loss will be used for classification problems.

We have tested extensively both in regression and classification tasks, scaling from simplified settings to realistic models and datasets. The regression tasks are with the Abalone and Diamonds datasets from the UCI repository (Dua & Graff, 2017), as well as with the popular "House Sales in King County, USA" (KC_House) dataset from the Kaggle competition website (harlfoxem, 2014). For the classification task we used the CIFAR-10, CIFAR-100 (Krizhevsky & Hinton, 2009), SVHN (Netzer et al., 2011) and FashionMnist (Xiao et al., 2017) datasets.

In all experiments, we split the dataset into three sets. These three are the typical prediction tasks sets: training set $Z_{\text{train}}$, testing set $Z_{\text{test}}$, and validation set $Z_{\text{validation}}$. For the regression setting, our experimental setup requires an extra set: a large sample set called "true" set $Z_{\text{true}}$, that is used to approximate the complete data distribution, and is used so as to estimate the Moment term. We use Monte Carlo sampling to estimate the Moment term ($f \sim \pi$ and $X', Y' \sim \mathcal{D}$), and the Empirical Risk term ($f \sim \hat{\rho}$). For the isotropic Laplace approximation, and a Gaussian isotropic prior, the KL divergence has a simple analytical expression $\mathrm{KL}(\hat{\rho}||\pi) = \frac{1}{2}\left(d\frac{\sigma^2_{\hat{\rho}}(\lambda)}{\sigma^2_{\pi}} + \frac{1}{\sigma^2_{\pi}}\|\mathbf{w}_{\hat{\rho}} - \mathbf{w}_{\pi}\|^2 - d - d\ln\sigma^2_{\hat{\rho}}(\lambda) + d\ln\sigma^2_{\pi}\right)$. PAC-Bayes bounds require correct control of the prior mean as the $\ell_2$ distance between prior and posterior means in the KL term is often the dominant term in the bound. To control this distance, we follow a variation of the approach in Dziugaite et al. (2021) to constructing our classifiers. We first use $Z_{\text{train}}$ to find a prior mean $\mathbf{w}_{\pi}$. We then set the posterior mean equal to the prior mean $\mathbf{w}_{\hat{\rho}} = \mathbf{w}_{\pi}$ but evaluate the r.h.s of the bounds on $Z_{\text{validation}}$. Note that in this way $\|\mathbf{w}_{\hat{\rho}} - \mathbf{w}_{\pi}\|_2^2 = 0$, while the bound is still valid since the prior is independent from the evaluation set $X, Y = Z_{\text{validation}}$. For the Abalone, Diamonds and KC_House experiments, we use fully connected networks with 2 hidden layers with 100 dimensions, followed by the ReLU activation function, and a final Softmax activation. For the CIFAR-10, CIFAR-100, and SVHN datasets, we use a WideResNet22 (Zagoruyko & Komodakis, 2016), with Fixup initialization (Zhang et al., 2019). For the FashionMnist dataset, we use a convolutional architecture with three convolutional layers, followed by two fully connected non-linear layers. More details on the experimental setup can be found in the Appendix.

### 3.1 Regression experiments

We find ten MAP estimates for the neural network weights of the Abalone, Diamonds and KC_House datasets by training on $Z_{\text{train}}$ using Stochastic Gradient Descent (SGD) with stepsize $\eta = 10^{-3}$ for ten epochs. We then fit an Isotropic Laplace approximation to each MAP estimate using $Z_{\text{validation}}$. For different values of $\lambda$ we then estimate the Alquier bound (Theorem 1) using $X, Y = Z_{\text{validation}}$,

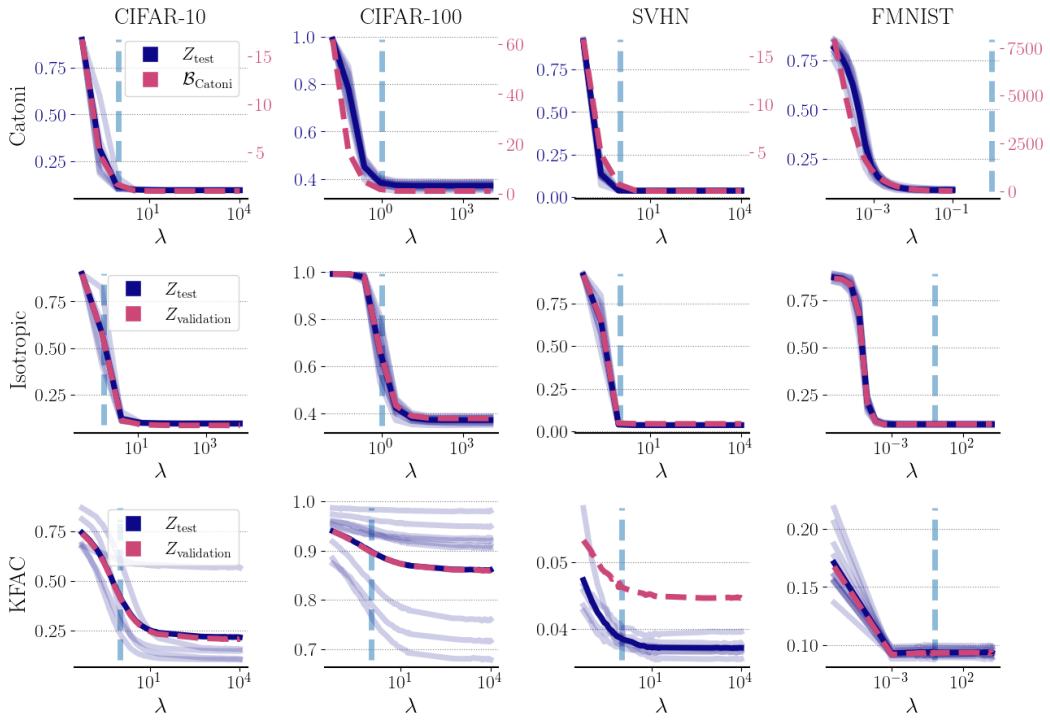


Figure 3: Test 0-1 Loss mean, as well as 10 MAP trials, along with the generalization certificate (we denote $\lambda = 1$ by ): $\mathcal{B}_{\text{Catoni}}$ PAC-Bayes bound (top), standard Isotropic Laplace posterior (middle) and standard KFAC (bottom). The $\mathcal{B}_{\text{Catoni}}$ PAC-Bayes bound closely tracks the test 0-1 Loss. For the standard Isotropic and KFAC posteriors the test and validation 0-1 Loss behave similar to the Catoni case, with a rapid improvement as $\lambda \uparrow$ followed by a plateau. Coldest posteriors $\lambda \gg 1$ are always best.

as well as the *test* NLL of the posterior predictive on $Z_{\text{test}}$. We take a grid over prior variances $\sigma_\pi^2$, and we present results for $\sigma_\pi^2 = 0.005$ although the behaviour is similar for the other prior values.

We plot the results for all datasets in Figure 2. Somewhat surprisingly, the test NLL always decreases with colder posteriors up to the point where the classifier is essentially deterministic. The $\mathcal{B}_{\text{Alquier}}$ bound correlates tightly with this behaviour. We plot this correlation in Figure 1(a). These results are somewhat surprising, in that we would expect there to be a minimum in the curves, such that *some* posterior variance $\sigma_{\hat{\rho}} \geq 0$ gives better test results than the MAP estimate. We might think that these results are due to the poor (Isotropic) approximation to the posterior, however as will we see in the next section this behaviour carries over to other approximations to the posterior.

### 3.2 Classification Experiments

We find ten MAP estimates for the neural network weights of the CIFAR-10, CIFAR-100, SVHN and FMNIST datasets by training on $Z_{\text{train}}$ using SGD. We then fit an Isotropic Laplace approximation to each MAP estimate using $X, Y = Z_{\text{validation}}$. For different values of $\lambda$ we then estimate the Catoni bound (Theorem 2) using $Z_{\text{validation}}$. We also estimate the *test* 0-1 Loss, negative log-likelihood (NLL) and the Expected Calibration Error (ECE) (Naeini et al., 2015) of the posterior predictive on $Z_{\text{test}}$. We use the prior variance $\sigma_\pi^2 = 0.1$, as optimizing the marginal likelihood leads to $\sigma_\pi^2 \approx 0$ which is not relevant for BNNs. We also test two standard setups of increasing difficulty. First, the standard "Isotropic" case where we fit the Laplace on $Z_{\text{train}}$. Second, the KFAC case where we fit the Laplace on $Z_{\text{train}}$ and also choose the prior through the marginal likelihood. In both of these last two cases, we estimate the evaluation metrics on the validation set $Z_{\text{validation}}$ as from the literature we know that any PAC-Bayes bound will be vacuous (larger than 1) as we do not control $\|\mathbf{w}_{\hat{\rho}} - \mathbf{w}_\pi\|_2^2$.

We plot the results for all datasets in Figure 3. The Catoni bound correlates tightly with test 0-1 Loss for all datasets and we plot this correlation in Figure 1(b). Again, in terms of test 0-1 Loss, the MAP estimate (obtained where $\lambda \gg 1$ and the posterior is "coldest") is optimal. This bevaviour is replicated both in the "Isotropic" and "KFAC" cases. In the Laplace approximation literature for deep neural networks, there are various similar results hidden in plain sight and to the best of our knowledge *never directly addressed* (Antorán et al., 2022; Daxberger et al., 2021; Ritter et al., 2018).

The crucial point here is the choice of the *evaluation metric*. We plot in Figure 4 the Isotropic and KFAC cases for the NLL. Even without data augmentation and even when we optimize the prior variance using the marginal likelihood, we find that all three cases of temperatures (cold posterior, warm posterior, as well as posterior with $\lambda = 1$) can be optimal, for varying datasets. Unfortunately we cannot estimate the Alquier bound for this case, as we do not have access to a $Z_{\text{true}}$ set, so as to compute the Moment term. However, we see again that the test behaviour is dominated by a sharp improvement as we decrease the posterior variance ($\lambda \uparrow$) followed by a plateau. An optimal $\lambda$ strictly less than $+\infty$ (when it exists) results in only a relatively modest variation of the overall trend. Thus, we believe that our bounds would be informative even in a hypothetical scenario where they would not be able to capture these optimal $\lambda < +\infty$. We discuss the ECE results in the Appendix.

## 4 Effect of temperature parameter $\lambda$ on PAC-Bayes bound

In light of our empirical results, it would be interesting to derive an analytical form that elucidates the important variables that affect the bound. However, PAC-Bayes objectives are difficult to analyze theoretically for the non-convex case. Thus in the following we make a number of simplifying assumptions. The Laplace approximation with the Generalized Gauss-Newton approximation to the Hessian corresponds to a linearization of the neural network around the MAP estimate $\mathbf{w}_{\hat{\rho}} \in \mathbb{R}^d$ (Immer et al., 2021)

$$f_{\text{lin}}(\boldsymbol{x}; \mathbf{w}) = f(\boldsymbol{x}; \mathbf{w}_{\hat{\rho}}) + \nabla_{\mathbf{w}} f(\boldsymbol{x}; \mathbf{w}_{\hat{\rho}})^\top (\mathbf{w} - \mathbf{w}_{\hat{\rho}}). \tag{4}$$

When analyzing minima of the loss landscape linearization is reasonable even without assuming infinite width Zancato et al. (2020); Maddox et al. (2021). For appropriate modelling choices, we aim at deriving a bound for this linearized model.

We adopt the linear form (4) together with the Gaussian likelihood with $\sigma = 1$, yielding $\ell_{\text{nll}}(\mathbf{w}, \boldsymbol{x}, y) = \frac{1}{2}\ln(2\pi) + \frac{1}{2}(y - f(\boldsymbol{x}; \mathbf{w}_{\hat{\rho}}) - \nabla_{\mathbf{w}} f(\boldsymbol{x}; \mathbf{w}_{\hat{\rho}})^\top (\mathbf{w} - \mathbf{w}_{\hat{\rho}}))^2$. We also make the following modeling choices

- Prior over weights: $\mathbf{w} \sim \mathcal{N}(\mathbf{w}_\pi, \sigma_\pi^2 \mathbf{I})$.
- Gradients as Gaussian mixture: $\nabla_{\mathbf{w}} f(\boldsymbol{x}; \mathbf{w}_{\hat{\rho}}) \sim \sum_{i=1}^k \phi_i \mathcal{N}(\boldsymbol{\mu}_i, \sigma_{\boldsymbol{x}i}^2 \mathbf{I})$; note that this assumption should be plausible for *trained* neural networks, in that previous works have shown that per sample gradients with respect to the weights, at $\mathbf{w}_{\hat{\rho}}$, are clusterable (Zancato et al., 2020). We consider that a Gaussian Mixture model for these clusters is reasonable.
- Labeling function: $y = f(\boldsymbol{x}; \mathbf{w}_{\hat{\rho}}) + \nabla_{\mathbf{w}} f(\boldsymbol{x}; \mathbf{w}_{\hat{\rho}})^\top (\mathbf{w}_* - \mathbf{w}_{\hat{\rho}}) + \epsilon$, where $\epsilon \sim \mathcal{N}(0, \sigma_\epsilon^2)$.

Thus $y|\boldsymbol{x} \sim \mathcal{N}(f(\boldsymbol{x}; \mathbf{w}_{\hat{\rho}}) + \nabla_{\mathbf{w}} f(\boldsymbol{x}; \mathbf{w}_{\hat{\rho}})^\top (\mathbf{w}_* - \mathbf{w}_{\hat{\rho}}), \sigma_\epsilon^2)$. The assumption that $\mathbf{w}_*$ is close to $\mathbf{w}_{\hat{\rho}}$ is quite strong, and we furthermore argued in the previous sections that no single $\mathbf{w}$ is truly "correct". However we note that for fine-tuning tasks linearized neural networks work remarkably well (Maddox et al., 2021; Deshpande et al., 2021). It is therefore at least somewhat reasonable to assume the above oracle labelling function, in that for deep learning architectures good $\mathbf{w}$ that fit many datasets can be found close to $\mathbf{w}_{\hat{\rho}}$ in practical settings. We also assume that we have a deterministic estimate of the posterior weights $\mathbf{w}_{\hat{\rho}}$ *which we keep fixed*, and we model the posterior as $\hat{\rho} = \mathcal{N}(\mathbf{w}_{\hat{\rho}}, \sigma_{\hat{\rho}}^2(\lambda)\mathbf{I})$, similarly to our experimental section. Therefore estimating the posterior corresponds to estimating the variance $\sigma_{\hat{\rho}}^2(\lambda)$.

**Proposition 1** ($\mathcal{B}_{\text{approximate}}$)**.** *With the above modeling choices, and given a distribution $\mathcal{D}$ over $\mathcal{X} \times \mathcal{Y}$, real numbers $\delta \in (0, 1]$ and $\lambda \in (0, \frac{1}{c})$ with $c = 2n\sigma_{\boldsymbol{x}}^2\sigma_\pi^2$, with probability at least $1 - \delta$*

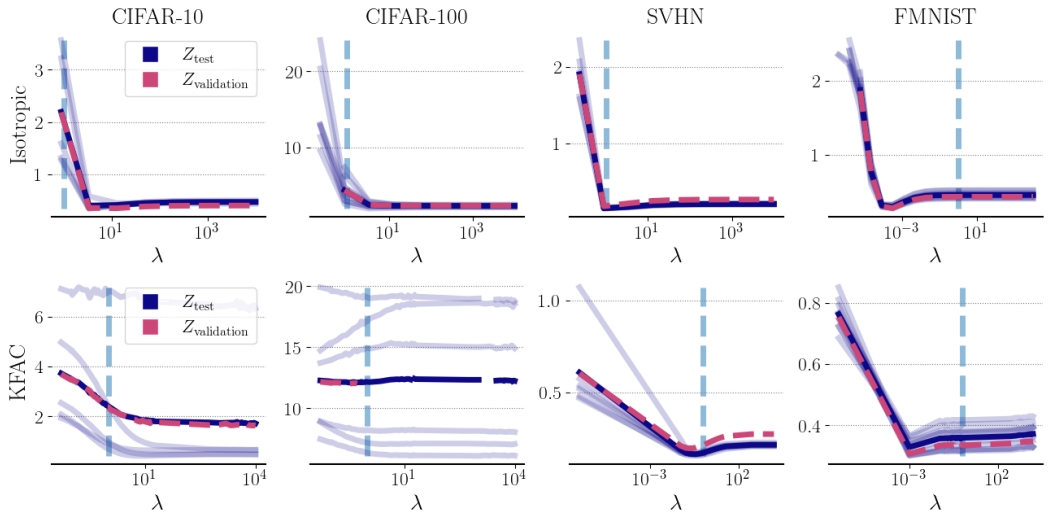


Figure 4: Test NLL ——— mean, as well as 10 MAP trials ——, along with the validation NLL - - - (we denote $\lambda = 1$ by - - -) for the Standard Isotropic Laplace posterior (top) and standard KFAC (bottom). The test and validation NLL show warm posteriors (FMNIST and SVHN KFAC), cold posteriors (CIFAR-10) and posteriors with $\lambda = 1$ (SVHN Isotropic). The general trend remains a rapid improvement as $\lambda \uparrow$ followed by a plateau, however the coldest posteriors $\lambda \gg 1$ are not always optimal contrary to the 0-1 Loss case.

*over the choice* $(X, Y) \sim \mathcal{D}^n$*, we have*

$$\mathbf{E}_{\mathbf{w}\sim\hat{\rho}}\mathcal{L}^{\ell_{\text{nll}}}_{\mathcal{D}}(\mathbf{w})$$
$$\leq \underbrace{\frac{\|\boldsymbol{y} - f(\mathbf{X};\mathbf{w}_{\hat{\rho}})\|_2^2}{2n} + \left(\frac{\lambda h}{d} + \frac{1}{\sigma_\pi^2}\right)^{-1}\frac{h}{2n} + \frac{1}{2}\ln(2\pi)}_{\text{Empirical Risk}} + \underbrace{\frac{\sigma_{\boldsymbol{x}}^2(\sigma_\pi^2 d + \|\mathbf{w}_*\|_2^2)}{1 - 2\lambda n\sigma_{\boldsymbol{x}}^2\sigma_\pi^2} + \sigma_\epsilon^2}_{\text{Moment}} +$$
$$\underbrace{\frac{1}{\lambda n}\left[\frac{1}{2}\left(\frac{d}{\sigma_\pi^2}\frac{1}{\frac{\lambda h}{d} + \frac{1}{\sigma_\pi^2}} + \frac{1}{\sigma_\pi^2}\|\mathbf{w}_{\hat{\rho}} - \mathbf{w}_\pi\|_2^2 - d - d\ln\frac{1}{\frac{\lambda h}{d} + \frac{1}{\sigma_\pi^2}} + d\ln\sigma_\pi^2\right) + \ln\frac{1}{\delta}\right]}_{\text{KL}}$$

*where* $h = \sum_i \sum_j (\nabla_{\mathbf{w}} f(\boldsymbol{x}_i; \mathbf{w}_{\hat{\rho}})_j)^2$ *is the curvature parameter, and* $\sigma_{\boldsymbol{x}}^2 = \sum_{j=1}^k \phi_j \sigma_{\boldsymbol{x}j}^2$ *is the posterior gradient variance.*

We now make a number of observations regarding Proposition 1. Here, $h$ is the trace of the Hessian under the Gauss–Newton approximation (without a scaling factor $n$). Under the PAC-Bayesian modeling of the risk, cold posteriors are the result of a complex interaction between various parameters resulting from 1) our *model* such as the prior variance $\sigma_\pi^2$ and prior mean $\mathbf{w}_\pi$ 2) our *data* $\sigma_{\boldsymbol{x}}^2$ and $\mathbf{w}_*$ (the curvature of the minimum $h$ and the MAP estimate $\mathbf{w}_{\hat{\rho}}$ depend on the deep neural network architecture, the optimization procedure and the data). A number of works have tried to identify the causes of the cold posterior effect (Noci et al., 2021; Fortuin et al., 2021), with often contradictory results, typically identifying sufficient but necessary conditions. Given the complex interactions in Proposition 1, our result might shed light on why pinpointing the exact cause is difficult in practice.

## 5 Discussion

A number of interesting questions are raised by our results. How can we link our results to the MCMC setting? Which metrics are relevant for the cold-posterior effect? For which metrics and for which approximations to the curvature is the Laplace approximation relevant for modern deep learning? We intend to answer these in future work.

## REFERENCES


Ben Adlam, Jasper Snoek, and Samuel L Smith. Cold posteriors and aleatoric uncertainty. *ICML Workshop on Uncertainty and Robustness in Deep Learning*, 2020.

Laurence Aitchison. A statistical theory of cold posteriors in deep neural networks. In *International Conference on Learning Representations*, 2020.

Pierre Alquier, James Ridgway, and Nicolas Chopin. On the properties of variational approximations of Gibbs posteriors. *The Journal of Machine Learning Research*, 17(1):8374–8414, 2016.

Javier Antorán, David Janz, James U Allingham, Erik Daxberger, Riccardo Rb Barbano, Eric Nalisnick, and José Miguel Hernández-Lobato. Adapting the linearised laplace model evidence for modern deep learning. In *International Conference on Machine Learning*, pp. 796–821. PMLR, 2022.

Arsenii Ashukha, Alexander Lyzhov, Dmitry Molchanov, and Dmitry Vetrov. Pitfalls of in-domain uncertainty estimation and ensembling in deep learning. In *International Conference on Learning Representations*, 2019.

Gregor Bachmann, Lorenzo Noci, and Thomas Hofmann. How tempering fixes data augmentation in bayesian neural networks. *arXiv preprint arXiv:2205.13900*, 2022.

David Blackwell and Lester Dubins. Merging of opinions with increasing information. *The Annals of Mathematical Statistics*, 33(3):882–886, 1962.

Charles Blundell, Julien Cornebise, Koray Kavukcuoglu, and Daan Wierstra. Weight uncertainty in neural network. In *International Conference on Machine Learning*, pp. 1613–1622. PMLR, 2015.

Olivier Catoni. *PAC-Bayesian supervised classification: the thermodynamics of statistical learning*, volume 56 of *Monograph Series*. Institute of Mathematical Statistics Lecture Notes, 2007.

Thomas M Cover. *Elements of information theory*. John Wiley & Sons, 1999.

Erik Daxberger, Agustinus Kristiadi, Alexander Immer, Runa Eschenhagen, Matthias Bauer, and Philipp Hennig. Laplace Redux-Effortless Bayesian Deep Learning. *Advances in Neural Information Processing Systems*, 34, 2021.

Aditya Deshpande, Alessandro Achille, Avinash Ravichandran, Hao Li, Luca Zancato, Charless Fowlkes, Rahul Bhotika, Stefano Soatto, and Pietro Perona. A linearized framework and a new benchmark for model selection for fine-tuning. *arXiv preprint arXiv:2102.00084*, 2021.

Dheeru Dua and Casey Graff. UCI machine learning repository, 2017. URL http://archive.ics.uci.edu/ml.

Michael Dusenberry, Ghassen Jerfel, Yeming Wen, Yian Ma, Jasper Snoek, Katherine Heller, Balaji Lakshminarayanan, and Dustin Tran. Efficient and scalable Bayesian neural nets with rank-1 factors. In *International Conference of Machine Learning*, pp. 2782–2792. PMLR, 2020.

Gintare Karolina Dziugaite and Daniel M Roy. Computing nonvacuous generalization bounds for deep (stochastic) neural networks with many more parameters than training data. *Uncertainty in Artificial Intelligence*, 2017.

Gintare Karolina Dziugaite, Kyle Hsu, Waseem Gharbieh, Gabriel Arpino, and Daniel Roy. On the role of data in PAC-Bayes. In *International Conference on Artificial Intelligence and Statistics*, pp. 604–612. PMLR, 2021.

Vincent Fortuin, Adrià Garriga-Alonso, Florian Wenzel, Gunnar Rätsch, Richard Turner, Mark van der Wilk, and Laurence Aitchison. Bayesian neural network priors revisited. In *International Conference on Learning Representations*, 2021.

Pascal Germain, Francis Bach, Alexandre Lacoste, and Simon Lacoste-Julien. PAC-Bayesian theory meets Bayesian inference. *Advances in Neural Information Processing Systems*, 29, 2016.

Subhashis Ghosal, Jayanta K Ghosh, and Aad W Van Der Vaart. Convergence rates of posterior distributions. *Annals of Statistics*, pp. 500–531, 2000.

Peter Grünwald. The safe Bayesian. In *International Conference on Algorithmic Learning Theory*, pp. 169–183. Springer, 2012.

Peter Grünwald and John Langford. Suboptimal behavior of Bayes and MDL in classification under misspecification. *Machine Learning*, 66(2):119–149, 2007.

Peter Grünwald and Thijs Van Ommen. Inconsistency of Bayesian inference for misspecified linear models, and a proposal for repairing it. *Bayesian Analysis*, 12(4):1069–1103, 2017.

harlfoxem. Kaggle. https://www.kaggle.com/datasets/harlfoxem/housesalesprediction, 2014.

Alexander Immer, Maciej Korzepa, and Matthias Bauer. Improving predictions of Bayesian neural nets via local linearization. In *International Conference on Artificial Intelligence and Statistics*, pp. 703–711. PMLR, 2021.

Pavel Izmailov, Sharad Vikram, Matthew D Hoffman, and Andrew Gordon Gordon Wilson. What are Bayesian neural network posteriors really like? In *International Conference on Machine Learning*, pp. 4629–4640. PMLR, 2021.

Mohammad Khan, Didrik Nielsen, Voot Tangkaratt, Wu Lin, Yarin Gal, and Akash Srivastava. Fast and scalable Bayesian deep learning by weight-perturbation in ADAM. In *International Conference on Machine Learning*, pp. 2611–2620. PMLR, 2018.

Alex Krizhevsky and Geoffrey Hinton. Learning multiple layers of features from tiny images. *Citeseer*, 2009.

Frederik Kunstner, Philipp Hennig, and Lukas Balles. Limitations of the empirical fisher approximation for natural gradient descent. *Advances in neural information processing systems*, 32, 2019.

Sanae Lotfi, Pavel Izmailov, Gregory Benton, Micah Goldblum, and Andrew Gordon Wilson. Bayesian model selection, the marginal likelihood, and generalization. In *Proceedings of the 39th International Conference on Machine Learning*, volume 162 of *Proceedings of Machine Learning Research*, pp. 14223–14247. PMLR, 17–23 Jul 2022.

Wesley Maddox, Shuai Tang, Pablo Moreno, Andrew Gordon Wilson, and Andreas Damianou. Fast adaptation with linearized neural networks. In *International Conference on Artificial Intelligence and Statistics*, pp. 2737–2745. PMLR, 2021.

James Martens and Roger Grosse. Optimizing neural networks with Kronecker-factored approximate curvature. In *International conference on machine learning*, pp. 2408–2417. PMLR, 2015.

Andres Masegosa. Learning under model misspecification: Applications to variational and ensemble methods. *Advances in Neural Information Processing Systems*, 33:5479–5491, 2020.

David A McAllester. Some PAC-Bayesian theorems. *Machine Learning*, 37(3):355–363, 1999.

Aaron Mishkin, Frederik Kunstner, Didrik Nielsen, Mark Schmidt, and Mohammad Emtiyaz Khan. Slang: Fast structured covariance approximations for Bayesian deep learning with natural gradient. *Advances in Neural Information Processing Systems*, 31, 2018.

Warren R Morningstar, Alex Alemi, and Joshua V Dillon. PAC$^m$-Bayes: Narrowing the empirical risk gap in the misspecified Bayesian regime. In *International Conference on Artificial Intelligence and Statistics*, pp. 8270–8298. PMLR, 2022.

Seth Nabarro, Stoil Ganev, Adrià Garriga-Alonso, Vincent Fortuin, Mark van der Wilk, and Laurence Aitchison. Data augmentation in Bayesian neural networks and the cold posterior effect. In *Uncertainty in Artificial Intelligence*, pp. 1434–1444. PMLR, 2022.

Mahdi Pakdaman Naeini, Gregory Cooper, and Milos Hauskrecht. Obtaining well calibrated probabilities using Bayesian binning. In *Twenty-Ninth AAAI Conference on Artificial Intelligence*, 2015.

Yuval Netzer, Tao Wang, Adam Coates, Alessandro Bissacco, Bo Wu, and Andrew Y Ng. Reading digits in natural images with unsupervised feature learning. *arxiv*, 2011.

Lorenzo Noci, Kevin Roth, Gregor Bachmann, Sebastian Nowozin, and Thomas Hofmann. Disentangling the roles of curation, data-augmentation and the prior in the cold posterior effect. *Advances in Neural Information Processing Systems*, 34, 2021.

Hippolyt Ritter, Aleksandar Botev, and David Barber. A scalable Laplace approximation for neural networks. In *6th International Conference on Learning Representations*, volume 6. International Conference on Representation Learning, 2018.

Florian Wenzel, Kevin Roth, Bastiaan S Veeling, Jakub Swiatkowski, Linh Tran, Stephan Mandt, Jasper Snoek, Tim Salimans, Rodolphe Jenatton, and Sebastian Nowozin. How good is the Bayes posterior in deep neural networks really? *International Conference on Machine Learning*, 2020.

Han Xiao, Kashif Rasul, and Roland Vollgraf. Fashion-mnist: a novel image dataset for benchmarking machine learning algorithms. *arxiv*, 2017.

Sergey Zagoruyko and Nikos Komodakis. Wide residual networks. In *British Machine Vision Conference 2016*. British Machine Vision Association, 2016.

Luca Zancato, Alessandro Achille, Avinash Ravichandran, Rahul Bhotika, and Stefano Soatto. Predicting training time without training. *Advances in Neural Information Processing Systems*, 33: 6136–6146, 2020.

Chen Zeno, Itay Golan, Ari Pakman, and Daniel Soudry. Why cold posteriors? on the suboptimal generalization of optimal Bayes estimates. In *Third Symposium on Advances in Approximate Bayesian Inference*, 2020.

Hongyi Zhang, Yann N Dauphin, and Tengyu Ma. Fixup initialization: Residual learning without normalization. In *International Conference on Learning Representations*, 2019.